0013-7227/96/$03.00/0
Endocrinology

Vol. 137, No. 1
Printed in U.S.A.

Differential Expression of Peroxisome Proliferator-Activated Receptors (PPARs): Tissue Distribution of PPAR-α, -β, and -γ in the Adult Rat*

OLIVIER BRAISSANT, FABIENNE FOUFELLE†, CHRISTIAN SCOTTO‡, MICHEL DAUÇA, AND WALTER WAHLI

Institut de Biologie Animale, Bâtiment de Biologie, Université de Lausanne (O.B., F.F., W.W.), CH-1015 Lausanne, Switzerland; Laboratoire de Biologie Cellulaire du Développement, Université de Nancy I, Faculté des Sciences (C.S., M.D.), F-54506 Vandoeuvre-les-Nancy, France; and Glaxo Institute for Molecular Biology (W.W.), Geneva, Switzerland

ABSTRACT

Peroxisome proliferator-activated receptors (PPARs) are members of the nuclear hormone receptor superfamily that can be activated by various xenobiotics and natural fatty acids. These transcription factors primarily regulate genes involved in lipid metabolism and also play a role in adipocyte differentiation. We present the expression patterns of the PPAR subtypes in the adult rat, determined by *in situ* hybridization using specific probes for PPAR-α, -β and -γ, and by immunohistochemistry using a polyclonal antibody that recognizes the three rat PPAR subtypes. In numerous cell types from either ectodermal, mesodermal, or endodermal origin, PPARs are coexpressed, with relative levels varying between them from one cell type to the other. PPAR-α is highly expressed in hepatocytes, cardiomyocytes, enterocytes, and the proximal tubule cells of kidney. PPAR-β is expressed ubiquitously and often at higher levels than PPAR-α and -γ. PPAR-γ is expressed predominantly in adipose tissue and the immune system. Our results suggest new potential directions to investigate the functions of the different PPAR subtypes. (*Endocrinology* **137:** 354–366, 1996)

PEROXISOME proliferator-activated receptors (PPARs) are nuclear receptors that are closely related to the thyroid hormone and retinoid receptors (1, 2). To date, three subtypes of PPARs have been described in amphibians, rodents, and humans: PPAR-α, -β (also called δ or NUC-1), and -γ (3–8). PPARs were first shown to be activated by substances that induce peroxisomal proliferation (3, 7). Further investigation revealed that natural fatty acids are also potent activators of PPARs (8, 9). No direct interaction of PPARs with either peroxisome proliferators or fatty acids has been described so far, leaving open the possibility that these activators are not *bona fide* PPAR ligands, with the exception, however, of an antidiabetic, thiazolidinedione (BRL 49653), which is a high affinity ligand of PPAR-γ (10).

The PPAR target genes encode enzymes involved in peroxisomal and mitochondrial β-oxidation and ketone body synthesis, as well as P450–4A6 fatty acid ω-hydroxylase, fatty acid binding proteins, apolipoproteins, lipoprotein lipase, malic enzyme, and phosphoenolpyruvate carboxykinase (reviewed in Ref. 1). Thus, PPARs play a key role in lipid metabolism and homeostasis. Peroxisomes participate in these processes, especially in liver, retina, heart cardiomyocytes, epithelial cells from kidney proximal tubules, and enterocytes (11). Cardiomyocytes and epithelial cells of kidney proximal tubules almost exclusively use fatty acids as energy source and are dependent on an efficient peroxisomal β-oxidation pathway for long-chain fatty acid catabolism (11, 12). Similarly, enterocytes of the intestinal villi display a very high peroxisomal β-oxidation activity (13). In the central nervous system (CNS), the fuel source for neurons is glucose (with very little participation of ketone bodies), in contrast to glial cells and especially astrocytes, which use a very high proportion of fatty acids (14). The structural role of fatty acids in brain membranes (axons, dendrites, and glial processes) is crucial for the nerve cell specific functions. Furthermore, the CNS needs efficient transport systems for trafficking and recycling lipids. In all tissues, membranes constitute important storage sites for arachidonic acid, which together with its metabolites (prostaglandins, leukotrienes, and thromboxanes), act as local hormones. Interestingly, arachidonic acid is a potent activator of PPARs (8, 9). Finally, adipose tissue plays key roles in lipid homeostasis and energy balance. Adipocytes can store lipids as triglycerides and release them as FFA, depending on the nutritional status and energy expenditure of the organism. It has recently been shown that PPAR-γ is a key transcription factor involved in adipogenesis (15, 16).

The roles of PPARs in gene regulation have been studied primarily in liver and adipose tissue (1). However, the PPAR genes are differentially expressed in a wide range of tissues in the adult organism (3, 4, 17, 18). The increasing awareness of the importance of PPARs in lipid metabolism led us to analyze their expression at the tissue level in a wide range of

Received August 1, 1995.
Address all correspondence and requests for reprints to: Walter Wahli, Institut de Biologie Animale, Bâtiment de Biologie, Université de Lausanne, CH-1015 Lausanne, Switzerland.
* This work was funded by the Etat de Vaud and the Swiss National Science Foundation.
† Supported by a fellowship from the European Molecular Biology Organization.
‡ Supported by the Ministère de l'Enseignement Supérieur et de la Recherche.

organs of the adult rat. *In situ* hybridization and immunohistochemical analysis, using specific probes for each of the rat PPARs (α, β, and γ), and one polyclonal antibody recognizing all three subtypes, allowed us to identify cell populations differentially expressing these receptors in the adult rat. Our observations suggest several new directions to investigate PPAR implications in lipid metabolism.

Materials and Methods

Cloning of PPAR-α, -β, and -γ complementary DNA (cDNA)

A cDNA comprising part of the D and E domains of the rat PPAR-α (nucleotides 1049–1766, Ref. 8) was obtained as described (19). A shorter 390-bp *Xba*I-*Rsa*I fragment (nucleotides 1377–1766) was cloned into the pBluescript KS+ and SK$^+$ vectors (Stratagene, Heidelberg, Germany) to obtain the recombinant plasmids pKS+/PPAR-α and pSK$^+$/PPAR-α.

A cDNA comprising part of the A/B domain of the rat PPAR-β was obtained by reverse transcription coupled to PCR, using primers derived from the mouse PPAR-β cDNA sequence (4). The first cDNA strand was synthesized from 10 μg of total RNA from adult rat brain using the mouse mammary leukemia virus-RT (GIBCO BRL, Gaithersburg, MD) and the primer β-down (5′-GGGAGGAATTCTGGGAGAGGTCTGCACAGC-3′, hybridizing at the 3′ end of the A/B domain of PPAR-β). The cDNA was then subjected to PCR amplification with the primers β-down and β-up (5′-GTCATGGATCCGCCACAGGAGGAGACCCCT-3′, hybridizing at the 5′-end of the A/B domain) using the *Taq* polymerase (GIBCO BRL). Amplification was carried out by 40 cycles at 95 C for 1 min 30 sec, 55 C for 2 min, and 72 C for 1 min, followed by an extension step at 72 C for 8 min. The PCR reaction mixture was subsequently treated with proteinase K (20), phenol/chloroform-extracted, ethanol-precipitated, and digested with *Eco*RI and *Bam*HI. The resulting insert (135 bp long, 96% homologous to the mouse PPAR-β, Ref. 4) was purified on agarose gel and cloned into the pBluescript KS+ and SK$^+$ vectors to obtain the recombinant plasmids pKS+/PPAR-β and pSK$^+$/PPAR-β.

A cDNA comprising part of the A/B and C domains of the rat PPAR-γ was obtained from 10 μg of total RNA from adult rat brown adipose tissue by reverse transcription coupled to PCR, as described above. The primers used, derived from the mouse PPAR-γ cDNA sequence (17), were γ-down (5′-TATCATAAATAAGCTTCAATCGGATGGTTC-3′, hybridizing in the C domain of the rat PPAR-γ) and γ-up (5′-GAGATGGAATTCTGGCCCACCAACTTCGG-3′, hybridizing in the A/B domain). After purification (see above), the PCR fragment was digested with *Eco*RI and *Hind*III and the resulting insert (403 bp long, 96% homologous to the mouse PPAR-γ, Ref. 17) was cloned into the pBluescript KS+ and SK$^+$ vectors to obtain the recombinant plasmids pKS+/PPAR-γ and pSK$^+$/PPAR-γ.

Riboprobe synthesis

Figure 1A shows a schematic representation of the riboprobes synthesized. The plasmids were linearized as follows: pKS+/PPAR-α with *Xba*I, pSK$^+$/PPAR-α, pSK$^+$/PPAR-γ, and pKS+/PPAR-β with *Eco*RI, pKS+/PPAR-γ with *Hind*III, and pSK$^+$/PPAR-β with *Bam*HI. These were then gel isolated and used as templates for antisense and sense Digoxygenin- and [α-^{32}P]uridine triphosphate (UTP)-labeled riboprobes (Boehringer Mannheim, Mannheim, Germany, and Amersham Corp., Little Chalfont, UK, respectively). The transcription mixture included 1 mM ATP, GTP, and cytidine triphosphate, 0.7 mM UTP, 0.3 mM Digoxygenin-UTP, and 250 nM [α-^{32}P]UTP. T7 RNA polymerase was used at 1 U/μl. The [α-^{32}P]UTP was used to determine probe concentration (scintillation) and length (gel electrophoresis). After digestion of the DNA templates by RQI-DNase (Promega, Madison, WI), the RNA probes were purified by two ethanol precipitations and resuspended in diethylpyrocarbonate (DEPC; Fluka, Buchs, Switzerland)-treated water.

Tissue preparation and in situ hybridization analysis

Male and female adult Sprague-Dawley rats (300 g, BRL, Basel) were dissected, and all analyzed tissues, except white adipose tissue, were

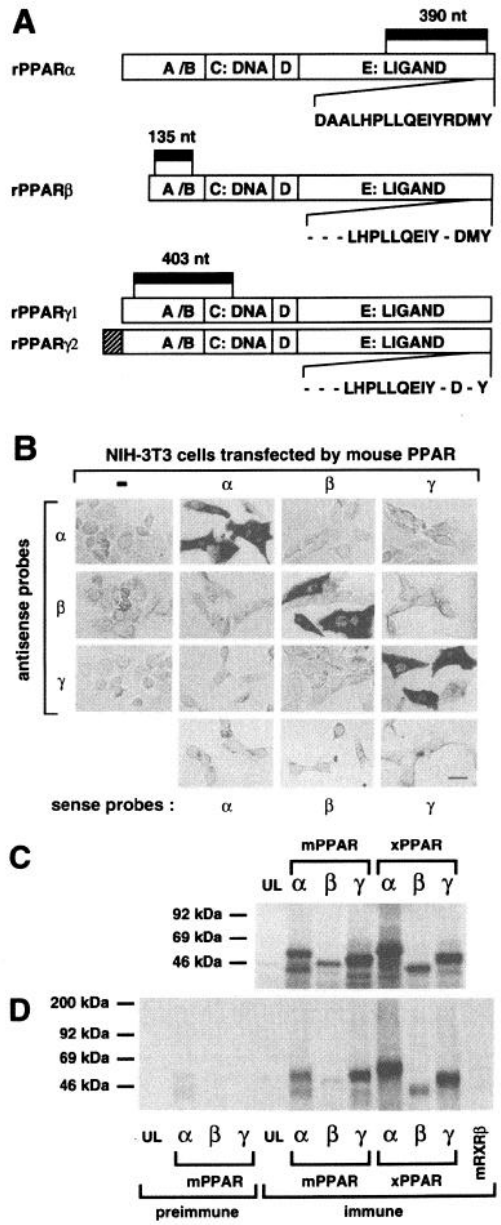

FIG. 1. Probes and antibody used to analyze expression of rPPAR-α, -β, and -γ by *in situ* hybridization and immunohistochemistry. A, Schematic representation. Functional domains (A-E) of PPARs are represented: C, DNA binding domain; E, ligand binding domain. *In situ* hybridization probes derived from corresponding cDNAs are indicated by *black bars*, and their length is given in nucleotides (nt). The last 16 amino acids of rPPAR-α recognized by the polyclonal antibody are indicated, as well as corresponding conserved amino acids of rPPAR-β and -γ, which are recognized as well. B, Hybridization specificity of rPPAR probes. Each rPPAR antisense probe was tested by *in situ* hybridization on NIH-3T3 cells transfected with either mPPAR-α, -β, or -γ. Endogenous levels of PPARs could not be detected on untransfected cells with the time of revelation used and hybridization was controlled with each sense probe. Time of revelation for each dish was 2 h. *Bar*, 20 μm. C, SDS-PAGE analysis of *in vitro* translated mouse and *Xenopus* PPAR-α, -β, and -γ. Three microliters of lysate were loaded in each lane; UL, unprogrammed lysate. D, Recognition of PPAR-α, -β, and -γ by anti-PPAR-α antibody. Immunoprecipitation assay with *in vitro* translated mouse and *Xenopus* PPAR-α, -β, and -γ and mouse RXR-β. Each lane represents immunoprecipitation of 5 μl of *in vitro* translated product; UL: unprogrammed lysate.

immediately embedded in tissue freezing medium (Jung, Nussloch, Germany) and frozen in isopentane and dry ice. Tissues were kept at −80 C until use. Tissue sections (12 μm thick) were cut (−35 C, Reichert and Jung Frigocut, Nussloch, Germany) and mounted on poly-L-lysinated slides. White adipose tissue was dehydrated through EtOH 70% (twice for 30 min), EtOH 95% (twice for 30 min), EtOH 100% (twice for 30 min), and xylol (twice for 30 min) and embedded in three successive baths of paraplast (58 C, Sherwood Medical, Athy, Ireland). After solidification, white adipose tissue sections were cut (12 μm thick at room temperature), mounted on poly-L-lysinated slides, air-dried overnight, and rehydrated through xylol (twice for 5 min), EtOH 100% (twice for 2 min), EtOH 95% (twice for 2 min), and DEPC-treated water (twice for 2 min). All sections were fixed 10 min in 4% paraformaldehyde-PBS, incubated twice for 15 min in PBS containing 0.1% active DEPC, and equilibrated 15 min in 5× SSC. Sections were prehybridized 2 h at 58 C in 50% formamide, 5× SSC, 40 μg/ml salmon sperm DNA, and hybridized 40 h at 58 C in the same mixture containing antisense or sense riboprobes at 400 ng/ml. Sections were washed 30 min in 2× SSC (room temperature), 1 h in 2× SSC (65 C), 1 h in 0.1× SSC (65 C), and equilibrated 5 min in Buffer 1 (100 mM Tris-HCl and 150 mM NaCl, pH 7.5). Sections were then incubated with alkaline phosphatase-coupled antidigoxygenin antibody (Boehringer Mannheim) diluted 1:5000 in Buffer 1 containing 0.5% blocking reagent (Boehringer Mannheim). Excess antibody was removed by two 15-min washes in Buffer 1, and sections were equilibrated 5 min in Buffer 2 (100 mM Tris-HCl, 100 mM NaCl, and 50 mM $MgCl_2$, pH 9.5). Revelation was performed at room temperature for 1 to 3 days in Buffer 2 containing 4-nitro blue tetrazolium chloride and X-phosphate (Boehringer Mannheim). Revelation was stopped by a 10-min wash in 10 mM Tris-HCl and 1 mM EDTA (pH 8.0), and slides were dehydrated and mounted (Eukitt, O. Kindler GmbH & Co., Freiburg, Germany). To ascertain the specificity of hybridization, sense probes for the PPAR genes (same length, guanosine and cytidine content and specific activity as the antisense probes) were used, and competition *in situ* hybridization experiments with a 100-fold excess of cold antisense probes were performed.

Cell culture

NIH-3T3 cells were cultured in DMEM containing 10% FCS (GIBCO BRL) and transfected at 80% confluence by electroporation (Bio-Rad Labs., Hercules, CA). Each dish (1×10^6 cells) received 10 μg of either mPPAR-α, -β, or -γ cloned in pSG5 (Stratagene), and 7.5 μg pBluescript KS+ (Stratagene) as a carrier. *In situ* hybridization was performed 48 h after transfection as described above, with the addition of 0.3% Triton X-100 (Sigma Chemical Co., St. Louis, MO) in the hybridization and antidigoxygenin antibody-containing buffers.

Immunohistochemistry

A rabbit polyclonal antibody raised against the 16 carboxy-terminal amino acids of rat PPAR-α (Fig. 1A and Scotto C, Hihi M, Mahfoudi A, Keller JM, Schohn H, Wahli W, and Dauça M, manuscript in preparation) was used in the immunohistochemistry studies. The preimmune serum was used as a control, as well as another nonimmune serum. Cryosections (12 μm thick) were fixed for 15 min in 4% paraformaldehyde-PBS, permeabilized 5 min in 1% Triton X-100 and 4% paraformaldehyde-PBS, and washed twice for 5 min in PBS. Sections were then incubated (1 h at room temperature) with the primary antibody (anti-PPAR-α) or the preimmune serum diluted 1:100 in PBS containing 0.1% FCS as a blocker. Sections were washed twice for 15 min in PBS and incubated (1 h at room temperature) with the secondary antibody (goat antirabbit IgG, tetramethyl-rhodamine isothiocyanate conjugated; Sigma) diluted 1:100 in PBS containing 0.1% FCS as a blocker. Sections were washed twice for 15 min in PBS and mounted in fluoprep medium (BioMérieux, Marcy, France).

Immunoprecipitation assay

In vitro translation of mouse PPAR-α-pSG5, mPPAR-β-pSG5, mPPAR-γ-pSG5, *Xenopus* PPAR-α-pSG5, xPPAR-β-pSG5, xPPAR-γ-pSG5, and mouse retinoid X receptor β (mRXR-β)-pSG5 plasmids was performed using reticulocyte lysate (Promega) as recommended by the manufacturer. Proteins were labeled with L-[^{35}S]methionine (Amersham). *In vitro* translated products were analyzed by SDS-PAGE by loading equal amounts (3 μl) lysates in each lane (Fig. 1C). Five hundred microliters protein A-Sepharose (Pharmacia) slurry were washed five times in equilibration buffer (10 mM Tris-HCl, pH 7.5, 1 mM EDTA, 1 mM dithiothreitol, 1 mM phenylmethylsulphonyl fluoride, 1 μg/ml pepstatin, and 1 μg/ml leupeptin) and were then incubated overnight with 50 μl unprogrammed reticulocyte lysate. Five microliters of translation product were used in each immunoprecipitation reaction, inbubated 2 h on ice in 50 μl incubation buffer (equilibration buffer, 40 mM KCl) containing either the anti-PPAR-α antibody or the preimmune serum at the same dilution. Fifty microliters protein A-Sepharose slurry were then added, and the complexes were immunoprecipitated 1 h at 4 C with continuous agitation. The immunoprecipitated complexes were washed five times in NET-N buffer (20 mM Tris-HCl, pH 8.0, 0.5% Nonidet P-40, 100 mM NaCl, and 1 mM dithiothreitol), resuspended in SDS sample buffer, and analyzed by SDS-PAGE (Fig. 1D).

Histological analysis

In situ hybridization and immunohistochemistry slides were observed and photographed on an Axiophot microscope (Carl Zeiss SA, Zürich, Switzerland), equiped with Nomarski (*in situ* hybridization) and fluorescence (immunohistochemistry) optics.

Results

Probe and antibody specificity

As a first step in the expression analyses of the different PPAR subtypes, we verified that the signals obtained were specific for the different forms of PPARs and not a consequence of a cross-hybridization or cross-reaction between related members of the superfamily. To mimic as closely as possible the *in situ* hybridization conditions, the specificity of the PPAR riboprobes (Fig. 1A) was verified by transfecting NIH-3T3 cells with either mPPAR-α, -β, or -γ. Between mouse and rat, the PPAR homologous regions presented 96% nucleotide identity, which does not affect the hybridization under the conditions used. In Fig. 1B we show that the three riboprobes directed against rPPAR-α, -β, or -γ were indeed specific for each of the PPAR forms. The endogenous PPAR level of the NIH-3T3 cells was not detectable with the time of revelation used (Fig. 1B). The specificity of the *in situ* hybridization experiments was also controlled with sense probes for each of the three PPARs, which gave no signal either on NIH-3T3 cells transfected with the mouse PPARs (Fig. 1B) or on adult rat tissue sections (Fig. 3J, PPAR-α; Fig. 6N, PPAR-β; Fig. 5O, PPAR-γ). Competition with a 100-fold excess of cold antisense probes abolished the signals (data not shown). Furthermore, the specificity of the antisense signals was corroborated by the occurrence of cell populations expressing different amounts of the three PPAR subtypes (see below).

The antibody used in this study was raised against the 16 last amino acids of rPPAR-α (all conserved in rat, mouse, human, and *Xenopus*). In rodents, as well as in *Xenopus*, 12 and 11 of the 16 last amino acids of PPAR-α are conserved in PPAR-β and PPAR-γ, respectively (Fig. 1A). Figure 1C shows that the translation efficiency of the different *in vitro* synthesized PPAR messenger RNAs varies. mPPAR-β and xPPAR-β are obtained in relatively low amounts compared with PPAR-α and -γ. Figure 1D demonstrates that the anti-PPAR-α antibody recognized the three forms of PPARs, either from mouse or *Xenopus*. All subtypes were recognized

equally well because the amounts of precipitated proteins were proportional to the amounts of *in vitro* translated PPARs used in the immunoprecipitation assay. Furthermore, this antibody was specific for PPARs, because it did not recognize another member of the nuclear hormone superfamily, mRXR-β. Using the preimmune serum as a control, no signal was obtained (Fig. 1D). The expression pattern of the PPAR proteins as determined by immunohistochemistry confirmed the *in situ* hybridization results. The cross-reactivity of the anti-PPAR-α antibody toward the different subtypes of PPARs was confirmed in cells expressing only one of the PPAR transcripts, such as PPAR-β in the Purkinje cells, which presented a high nuclear signal by immunohistochemical analysis (Fig. 2, H and I). Cells negative in *in situ* hybridization experiments, such as the intestinal smooth muscular cells, were also negative in immunohistochemistry experiments. The preimmune serum (Fig. 5K) as well as another nonimmune serum (data not shown) did not present any specific signal on tissue sections either.

CNS

In the adult CNS, PPARs presented the same expression patterns from one individual to the other, without significant variation between sexes (four males and three females tested). PPAR-β was abundantly expressed in the whole nervous system, whereas PPAR-α was limited to olfactory bulbs, hippocampus, cerebellum, and retina. PPAR-γ was also

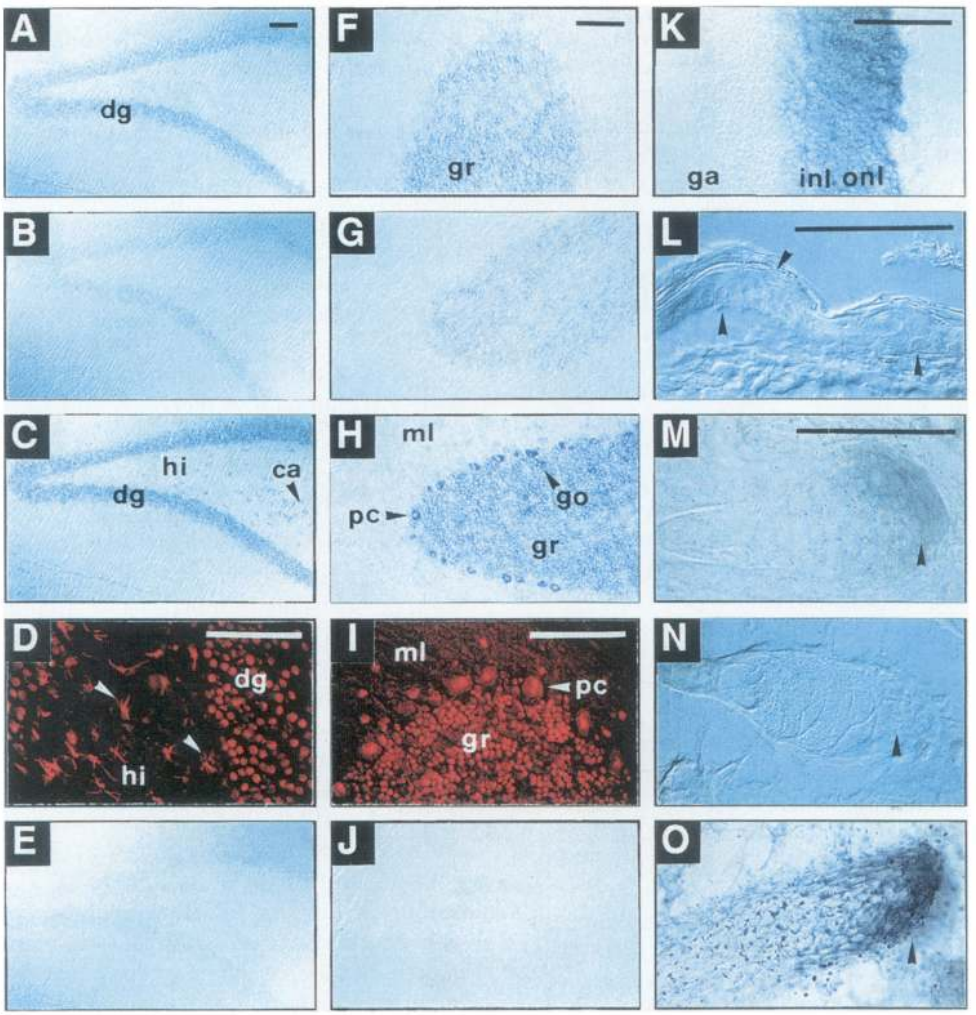

FIG. 2. Differential expression of rPPAR-α, -β, and -γ in CNS and epidermis: *in situ* hybridization and immunohistochemistry. A-E, Hippocampus. PPAR-α (A) and to a lesser extent PPAR-γ (B) are expressed in granular cells of the dentate gyrus (dg), whereas PPAR-β (C) is abundantly expressed in CA3 (end of the Ammon's horn, ca), the hilus (hi), and granular cells of the dentate gyrus. D, By immunohistochemical analysis, PPAR proteins are present in nuclei of granule cells of the dentate gyrus and the hilus. Fibers of astrocyte-like cells present a positive signal for PPARs (*arrows*). E, Control with a sense probe for PPAR-α. F-J, Cerebellum. PPAR-α (F) and -γ (G) are restricted to granular cells of cerebellum (gr), whereas PPAR-β (H) is abundantly expressed in granular, Golgi (go), and Purkinje (pc) cells, and to a lesser extent in neurons of the molecular layer (ml). I, Polyclonal antibody directed against PPAR-α, which recognizes also PPAR-β, labels granular and Purkinje cell nuclei, as well as nuclei in the molecular layer. J, Control with a sense probe for PPAR-α. K, Retina. PPAR-α is expressed in the inner (inl) and outer (onl) nuclear layers, but not in ganglion cells (ga). L, Epidermal keratinocytes (*arrow*) present no expression of PPARs in the adult rat. *In situ* hybridization with an antisense probe for PPAR-α. M-O, Sebaceous glands of epidermis. *In situ* hybridization; antisense probes for PPAR-α (M), PPAR-γ (N), and PPAR-β (O). PPAR-β transcripts are very abundant at the basis of sebaceous glands, whereas PPAR-α is weakly expressed, and PPAR-γ is not detected (*arrows*). *Bars*, 100 μm; except L-O, 50 μm.

present in the retina and was barely detectable in hippocampus and cerebellum. A detailed description of these patterns follows.

In the hippocampus, the PPAR-α transcript was present in CA1 and the granular cells of the dentate gyrus but was barely detectable in CA3 and the hilus (Fig. 2A). Signals for PPAR-γ were weak and limited to granular cells of the dentate gyrus (Fig. 2B). In contrast, PPAR-β was highly expressed in the dentate gyrus, CA1 to CA3 pyramids, and the hilus (Fig. 2C). Immunohistochemistry analyses corroborated the *in situ* hybridization results (Fig. 2D). In addition, our antibody stained cells in the hilus with an astrocyte-like pattern, showing a high level of protein expression in the radial extensions of these cells (see below).

In the cerebellum, the PPAR-α transcript was only present in the granular cells (Fig. 2F), whereas PPAR-β was abundantly transcribed in the Purkinje cells, the granular cells, the Golgi cells, and the interneurons of the molecular layer (Fig. 2H). The PPAR-γ transcript was expressed only at a low level in the granular layer (Fig. 2G). Immunohistochemistry confirmed the localization of the three forms of PPARs by staining the granular layer, the Purkinje cell layer, and the molecular layer (Fig. 2I).

In the retina, the three forms of PPARs were present in the inner and outer nuclear layers (Fig. 2K, PPAR-α), but only PPAR-γ was detectable in the ganglion cells (Table 1). In the other regions of the CNS, PPAR-β was ubiquitously expressed, particularly in giant cells such as pyramids of the telencephalic cortex (layers III and IV) and giant neurons in the pons, as well as in already described CA3 neurons in the hippocampus and Purkinje cells in the cerebellum (Table 1). In contrast, PPAR-α was restricted to olfactory bulbs and barely detectable in telencephalic cortex, nuclei from thalamus, hypothalamus, and midbrain. PPAR-γ was barely detectable in olfactory bulbs and vestibular nuclei of the pons (Table 1). Finally, cells from the choroid plexus that secrete the cerebrospinal fluid were positive for PPAR-α and -β but not -γ (Table 1 and data not shown).

With respect to cell types, PPARs were expressed in neurons but seemed to be absent from oligodendrocytes. No significant labeling was obtained in the white matter of cerebellum or corpus callosum (Table 1). Expression of PPAR-β in astrocytes was reflected by the astrocyte-like pattern produced in the hippocampal hilus by immunohistochemical analysis (even in the cell processes, Fig. 2D) and the PPAR-β *in situ* hybridization probe (Fig. 2C). These cells colocalized with cells expressing glial fibrillary acidic protein, an astrocyte-specific marker (data not shown). The *in situ* hybridization indicated that PPAR-α and -γ were not expressed at detectable levels in these cells (Fig. 2, A and B).

Epidermis

In the adult rat epidermis, the three forms of PPARs were not detected in the strata basale and spinosum (dividing keratinocytes) or the strata granulosum and corneum (nondividing keratinocytes) (Fig. 2L). In contrast, the base of the sebaceous glands expressed PPAR-α at low levels and PPAR-β abundantly, whereas PPAR-γ was not detectable (Fig. 2, M, O, and N, respectively).

Kidney, liver, and pancreas

In the adult kidney, the PPAR-α and -β transcripts were the most prominent, whereas PPAR-γ remained at a low level (Table 1). PPAR-α and γ (Fig. 3, A and B) were present only in the cortex, in the proximal part of the nephron (glomerulus and proximal tubule). PPAR-β was expressed in the cortex and the medulla at the level of glomeruli and proximal tubules (Fig. 3C), Henle's loops (Fig. 3D), distal tubules, and collecting ducts (data not shown). Interestingly, when abundantly expressed, the PPAR transcripts were concentrated in the perinuclear region (Fig. 3, A and C).

In the adult liver, the PPAR-α form was predominantly expressed, with variable levels between animals (10 animals tested, Fig. 3, F and G and Table 1). The PPAR-α transcript presented a perinuclear distribution (Fig. 3F) and was often present as a gradient, which was highly expressed in periportal hepatocytes and less expressed in pericentric hepatocytes (data not shown). PPAR-β was expressed evenly in the hepatic lobule (no gradient nor perinuclear localization, Fig. 3H). PPAR-γ was below the detection level in the animals tested. By immunohistochemical analysis, the PPAR localization was mainly nuclear, although a cytoplasmic signal was observed (Fig. 3I).

In the pancreas, PPARs were expressed at the same levels in the exocrine (acini) and endocrine (islets) parts of the gland. PPAR-β was prominent (Fig. 3M), whereas PPAR-α and -γ remained low (Fig. 3, K and L).

Digestive tract

The expression of PPARs did not vary significantly from one animal to another in the digestive tract. The receptors were present only in mucosa and submucosa, but not in the surrounding smooth muscular layers (Fig. 4, A-R and Table 1). Their expression increased from esophagus to duodenum and jejunum, whereas it decreased from duodenum to colon (Fig. 4, A-R and Table 1).

PPAR-α and -β were expressed in the keratinocytes bordering the esophagal lumen (Fig. 3O) and in the submucosa (Fig. 4, A and M). PPAR-α presented a very high expression at the basis of the gastric glands in the chief cells producing pepsinogen (Fig. 4, B and S). It was also expressed in the remaining mucosa, in mucus-secreting cells, and in parietal cells that secrete hydrochloric acid (Fig. 4B). PPAR-β was expressed homogeneously from the basis of the gastric glands to the lumen of the stomach (Fig. 4N). PPAR-γ was at very low levels in the esophagus and the stomach (Fig. 4, G-H). In the digestive tract as a whole, PPAR-α and -β presented their peaks of expression in duodenum and jejunum (Fig. 4, C, O, and T). PPAR-γ remained low in these two regions (Fig. 4I), where most of the phospholipids and triglycerides are absorbed. The expression of all three receptors decreased from jejunum to colon, where their transcripts were barely detectable (Fig. 4, D-F, J-L, and P-R). PPARs were not expressed in the duodenal Brünner's glands producing alkaline mucus.

TABLE 1. Differential expression of PPAR-α, PPAR-β, and PPAR-γ in the adult rat

	PPAR		
	α	β	γ
CNS			
Telencephalon			
Olfactory bulbs	+[a]	+++	±
Cortex	±	++	−
Hippocampus:			
CA1	+	+++	−
CA3	±	+++	−
Dentate gyrus	+	+++	±
Diencephalon			
Thalamic nuclei	±	++	−
Hypothalamic nuclei	±	+	−
Retina			
Inner nuclear layer	+++	+++	++
Outer nuclear layer	+++	+++	++
Ganglion cells	−	−	±
Midbrain			
Colliculi	±	+	−
Red nucleus	−	+++	−
Brainstem			
Vesticular nuclei	−	+++	±
Reticular formation	−	++	−
Cerebellum			
Molecular layer	−	+	−
Purkinje cells	−	+++	−
Granule cells	+	+++	±
Deep nuclei	−	++	−
Choroid plexus	++	+++	−
Epidermis			
Keratinocytes (from Stratum basale to Stratum corneum)	−	−	−
Sebaceous glands and hair follicles	+	+++	−
Kidney			
Glomeruli	+	++	±
Proximal tubules	+++	+++	+
Henle's loops	−	+++	−
Distal lobules	−	+++	−
Collecting ducts	−	++	−
Liver			
Hepatocytes	+/++++[b]	++	−
Pancreas			
Acini (exocrine)	+	++	+
Islets (endocrine)	+	++	+
Heart			
Cardiomyocytes	−/++[b]	−/++[b]	−
White adipose tissue	+	++	+++
Immune system			
Spleen			
White pulp	++	+++	++++
Red pulp	+	++	+++
Peyer's patches	++	+++	++
Digestive tract			
Smooth muscular layers	−	−	−
Esophagus			
Keratinocytes	++	++	+
Submucosa	++	++	++
Stomach			
Chief cells	++++	++	+
Parietal cells	+++	++	+
Mucus cells	+++	++	+
Duodenum			
Crypt enterocytes	++++	+++	++
Villi enterocytes	++++	+++	++
Gobelet cells	++++	+++	++
Brünner's gland	−	−	−
Jejunum crypts and villi	+++	+++	++
Ileum crypts and villi	+++	+++	++
Cecum	++	++	++

TABLE 1. Continued

	PPAR		
	α	β	γ
Colon	+	+	+
Genital system			
Testis			
Spermatogonia to spermatozoan	−	−	−
Sertoli cells	++	++++	±
Leydig cells	+	++	−
Ovary			
Follicular cells	++	++	+
Oocyte	−	−	−
Seminal gland epithelium	++	++	++
Uterus			
Cervix	++	++	±
Uterine glands	++	++	±
Fallopian duct epithelium	++	++	+

[a] −, absent; ±, barely detectable; +, weak expression; ++, moderate expression; +++, strong expression; ++++, very strong expression. PPAR levels of expression, indicated by − or + signs, reflect differences in signal intensities observed by optical microscopy. The number of + signs do not represent a strictly linear measure of mRNA levels.

[b] In liver (PPAR-α) and heart (PPAR-α and -β), expression varies between individuals.

Immune system, heart, and white adipose tissue

The immune system was tested for PPAR expression in the spleen and Peyer's patches. In the spleen, PPARs were expressed mostly in the white pulp (B lymphocyte proliferation centers) and to a lesser extent in the red pulp (phagocytosis of old and damaged red blood cells) (Fig. 5, A and B, and Table I). In the digestive tract, the Peyer's patches, which consist of lymphoid nodes, are present mostly in the ileum. These centers of undifferentiated B lymphocyte proliferation intensively expressed the three forms of PPARs (Fig. 5, D-F). By immunohistochemical analysis, the PPAR proteins were concentrated in the center of the lymphoid node, confirming the *in situ* hybridization results (Fig. 5G).

In the cardiomyocytes, PPAR-α and -β were expressed in variable amounts depending on the animal (seven animals tested; see levels of expression in Table 1). Interestingly, when present, these transcripts were concentrated in the perinuclear zone of the cardiomyocytes (Fig. 5H), as seen in kidney and liver. PPAR-γ, whose expression was low in the heart, could not be detected in the animals tested. By immunohistochemical analysis, the PPAR proteins were shown to be mainly concentrated in the nuclei of the heart muscular cells, although the cytoplasm presented a faint signal when compared with the preimmune serum (Fig. 5, J and K).

In the white adipose tissue, the three PPARs were expressed at different levels. PPAR-α was faint and its transcripts were concentrated in the perinuclear zone of adipocytes (Fig. 5L, *arrow*). PPAR-γ was the most abundant and detectable in the perinuclear zone (Fig. 5M, *arrow*) and the remaining part of the adipocyte cytoplasm, except for the lipid vacuole (Fig. 5M). PPAR-β presented an intermediate expression (Fig. 5N). These results corroborated and extended previous reports of Northern blot analyses (3, 18, 21).

Genital system

In testis, PPAR-β was the most abundantly transcribed of the three receptors. Its expression was especially high in the seminiferous tubules and in Leydig cells of the interstitial space (Fig. 6, C-D and F). PPAR-α was only weakly expressed (Fig. 6, A and B), and PPAR-γ was barely detectable. The *in situ* hybridization experiments presented a signal from the periphery of the seminiferous tubules to their center (except where mature spermatozoans were exposed in the lumen). Immunohistochemical analysis revealed a signal in a monocellular layer of nuclei at the periphery of the seminiferous tubules (Fig. 6, E and F). Thus, PPAR-α and -β seemed to be expressed mainly by Sertoli cells, which have their nuclei at the border of the seminiferous tubules, but extend their cytoplasm throughout the tubule wall from the periphery to the lumen. No signal was detected in spermatozoans.

In the ovary, PPAR-α and -β were highly expressed in the follicles (Fig. 6, I and J), whereas PPAR-γ remained low (Table 1). Inside the follicle no expression was detectable in the oocyte, whereas follicular cells presented a strong signal by *in situ* hybridization and immunohistochemical analysis (Fig. 6, I-K). This differs from Northern blot results obtained in *Xenopus*, where PPAR-α and -β are expressed in the oocyte (3).

In the rat gonads, PPARs were expressed in nurse cells (Sertoli cells and follicular cells of corona radiata) and sexual hormone-producing cells (Leydig cells and follicular cells of granulosa and theca) but were not detectable in the germ line. In the other genital organs, all three PPARs were well expressed, *e.g.* in the epithelium of the seminal glands (Fig. 6M and Table 1), the uterine cavity and glands (Fig. 6O and Table 1), and the fallopian duct (Table 1 and data not shown).

Discussion

Differential expression of PPARs

The three forms of PPAR are expressed in numerous cell types, from ectodermal, mesodermal, and endodermal origins (Table 1). In most tissues, PPARs are coexpressed with relative levels of each subtype varying from one cell type to the other. In the nervous system, we have localized PPARs in neurons and astrocytes but not in oligodendrocytes. This

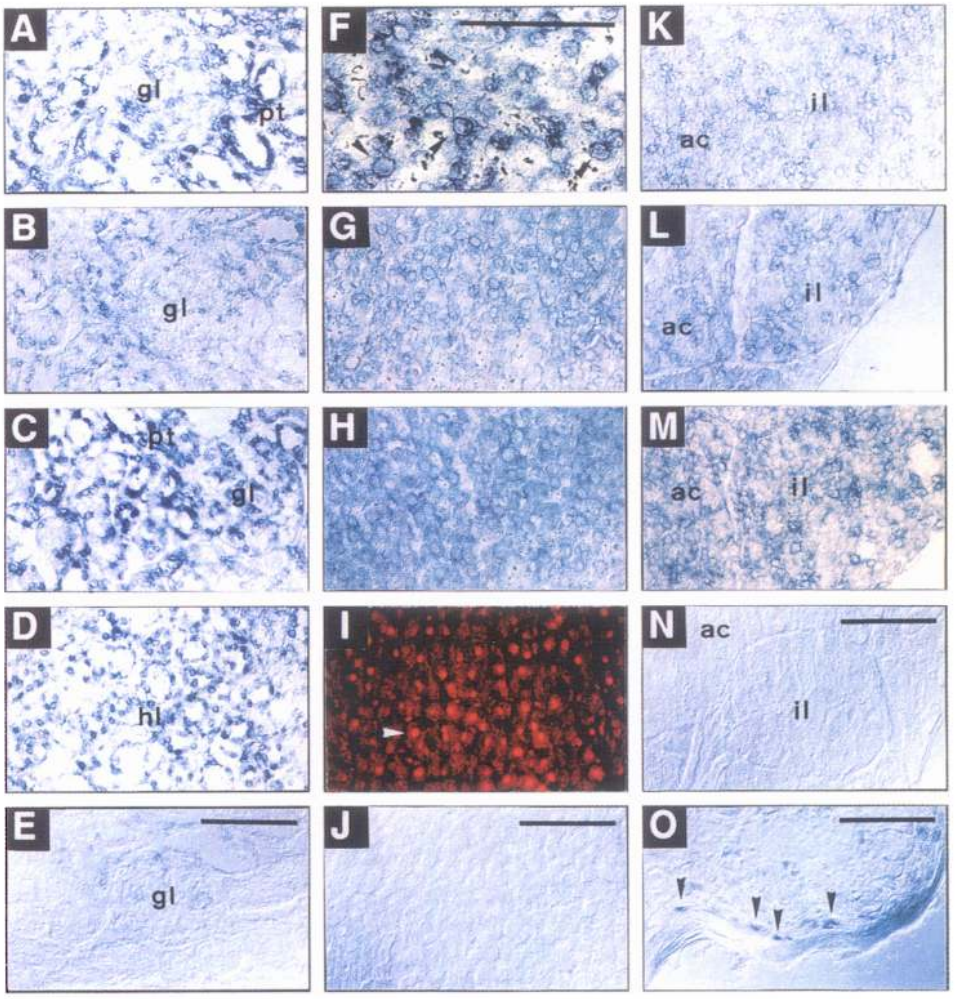

FIG. 3. Differential expression of rPPAR-α, -β, and -γ in kidney, liver, pancreas, and esophagus. A-E, Kidney. *In situ* hybridization. PPAR-α (A) is mainly expressed in the proximal tubules (pt), whereas PPAR-γ (B) is barely detectable, and PPAR-β (C-D) is abundant in glomeruli (gl), proximal tubules (pt), and Henle's loops (hl). E, Control with a sense probe for PPAR-α. F-J, Liver. *In situ* hybridization and immunohistochemistry. PPAR-α presents enormous variations of expression in the adult liver (F and G, two different females). When abundant, PPAR-α is highly concentrated in the perinuclear zone of hepatocytes (F, *arrow*). PPAR-β (H) presents a constant medium level of expression, whereas PPAR-γ is not detectable. I, Polyclonal antibody directed against PPAR-α labels mainly the hepatocyte nuclei (*arrow*). J, Control with a sense probe for PPAR-α. K-N, Pancreas. *In situ* hybridization. PPAR-α (K) and -γ (L) presents a medium level of expression, whereas PPAR-β (M) is more abundant. In all cases, levels of expression of a given PPAR are equivalent in exocrine (ac, acini) and endocrine (il, islets of Langerhans) pancreas. N, Control with a sense probe for PPAR-γ. O, esophagus. PPAR-α is expressed in proliferating, undifferentiated keratinocytes (*arrows*) from esophagal mucosa. *Bars*, 100 μm.

latter observation is not in agreement with the results of a recent study that showed expression of PPAR-α in the oligodendrocytes of the rat corpus callosum (22). PPARs are also expressed in cardiomyocytes, hepatocytes, adipocytes, pancreatic islets, and proliferating lymphocytes of the spleen and Peyer's patches. They are abundantly synthesized by epithelial cells, such as in exocrine pancreas, renal tubules, mucosa of digestive tract, seminal gland, uterine lumen and glands, and the fallopian duct. Moreover, the PPAR expression patterns do not differ significantly between males and females. Interestingly, the patterns are similar in cells of homologous functions in both male and female genitalia (nurse cells and sex hormone-producing cells), suggesting similar roles in both sexes.

To investigate the potential roles of PPARs in the different tissues, it is important to analyze the coexpression of both PPARs and RXRs, the required heterodimeric partners for the control of PPAR target genes (9, 23). In the adult mouse, RXR-α presents a strong expression in liver, kidney, and spleen, but it is also present in brain and heart. RXR-β has an ubiquitous distribution, but it is expressed at low levels in liver, intestine, and testis. RXR-γ presents a more restrictive pattern of expression, being localized only in kidney, liver, muscle, brain, and heart (24). Taken together, the PPAR and RXR expression patterns in the adult do not favor the occurrence of potential predominant functions for specific PPAR-RXR heterodimers in a given tissue. Although it has recently been shown that PPAR-γ2 interacts mainly with RXR-α in adipocytes (18, 25), the coexpression of PPARs and RXRs at various relative levels from one tissue to the other argues more favorably for differential heterodimerization between the multiple subtypes of these receptors. Indeed, it has been shown that all three PPAR subtypes can interact with either RXR-α, -β, or -γ isoforms on a peroxisome proliferator response element *in vitro* (4, 26).

We show that PPAR-α is abundantly expressed in cells with high mitochondrial and peroxisomal β-oxidation activity in liver, heart, proximal tubules of kidney, and intestinal mucosa (11, 13, 27), where it may regulate genes encoding mitochondrial and peroxisomal activities, as already demonstrated for hepatocytes (reviewed in Ref. 1). Cardiomyocytes and proximal tubules of kidney primarily use fatty acids as an energy source. In the intestine mucosa, peroxisomal β-oxidation is most active at the top of the villi (13), where the majority of fatty acid absorption takes place. Thus PPAR-α may regulate genes mainly involved in the catabolism of fatty acids. This potential key catabolic role for PPAR-α is in good agreement with the recent study of a mPPAR-α knockout mouse (28), which lost the inducibility of genes encoding peroxisomal and microsomal lipid-

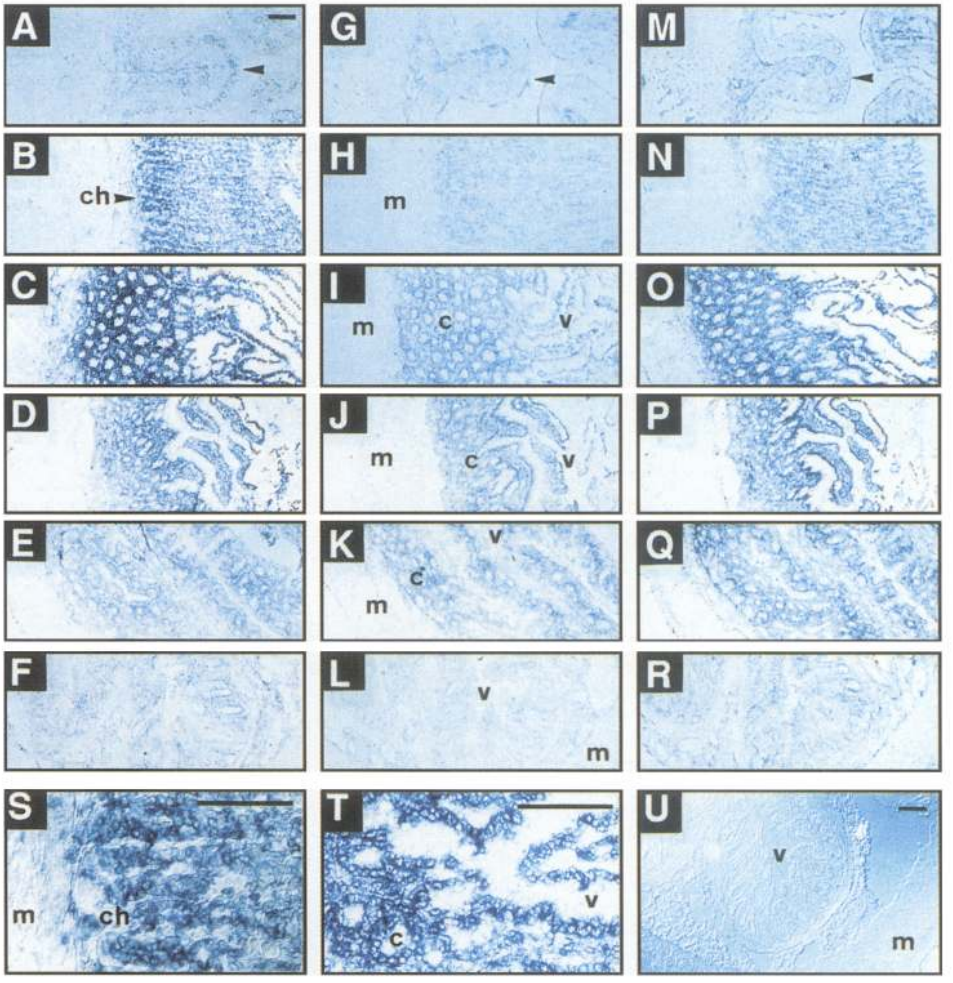

FIG. 4. Differential expression of rPPAR-α, -β, and -γ in digestive tract. A-F, S, and T, PPAR-α; G-L, PPAR-γ; and M-R, PPAR-β; and A, G, and M, esophagus. The three forms of PPARs are expressed in submucosa and keratinocytes (*arrow*) of stratified epithelium that is specific to rodent esophagus (see also Fig. 3O). B, H, N, and S, Stomach. In the gastric glands, PPAR-α is abundantly expressed in chief cells (ch). S, Higher magnification of chief cells expressing PPAR-α (ch). From duodenum (C, I, O, and T), ileum (D, J, and P), and cecum (E, K, and Q) to colon (F, L, R, and U), the three forms of PPARs are expressed in the mucosa (c, crypts; v, villi) according to a decreasing gradient, PPAR-α and -β being most abundant. T, Higher magnification of expression of PPAR-α in crypts (c) and villi (v) of the duodenum. Throughout the digestive tract, no expression of PPARs was observed in muscular layers (m). U, PPAR-γ sense control in colon. *Bars*, 100 μm.

metabolizing enzymes, such as acyl-CoA oxidase or cytochrome P450–4A1 ω-hydroxylase. The lack of the pleiotropic effects of peroxisome proliferators in the mPPAR-α knockout mouse (28) argues also for the strong involvement of PPAR-α in tissues presenting a high peroxisomal β-oxidation activity, such as hepatocytes, epithelial cells of kidney proximal tubules, or enterocytes.

In the liver, we observed particularly important variations of PPAR-α expression depending on the animal. This could be due to hormonal level differences between the adult rats used in this study, because the PPAR-α gene is regulated by glucocorticoids via the glucocorticoid receptor (19). Moreover, the PPAR-α gene has been shown *in vivo* to follow a circadian rhythm depending on the levels of glucocorticoids and to be up-regulated by stress conditions in liver but not in hippocampus (Lemberger T, Saladin R, Assimacopoulos F, Staels B, Wahli W, Auwerx J, submitted for publication). This could explain why PPAR-α expression varies in liver but remains more constant in other tissues.

We show in this study that PPAR-β is abundantly and ubiquitously expressed in the adult rat. To date, no specific function has been assigned to this PPAR subtype. However, it has recently been proposed that PPAR-β may modulate the activity of other PPARs, as it is capable of inhibiting PPAR-α activation, either by competition for the peroxisome proliferator response elements, or by titrating out a limiting factor required for the transcriptional activity of PPAR-α (29). Similarly, PPAR-γ has also been proposed to inhibit the transcriptional activity of PPAR-α (4). From this point of view, the ubiquitous expression of PPAR-β would be an efficient means to regulate the activity of the different PPARs, and their relative expression levels would lead to the activation of specific set of genes depending on the tissue.

We show that PPAR-γ is expressed abundantly in the white adipose tissue as well as in the immune system. Two isoforms of PPAR-γ have recently been described: PPAR-γ1 (17) and the adipose tissue-specific isoform PPAR-γ2, which differs from PPAR-γ1 only by 30 additional amino acids at the N-terminal extremity (18). The rPPAR-γ probe used in the *in situ* hybridization experiments recognizes both PPAR-γ1 and PPAR-γ2, as it is located in the region that is identical in the two isoforms (Fig. 1A). It has recently been shown that PPAR-γ2 regulates the aP2 gene encoding an adipocyte-specific fatty acid binding protein (18) as well as the phosphoenolpyruvate carboxykinase gene (25), which is responsible for glyceroneogenesis in adipocytes. Moreover, PPAR-γ can induce adipogenesis in fibroblasts (16). Recently, an antidiabetic, thiazolidinedione, which can induce adipogenesis in cultured fibroblasts, was shown to be a high affinity ligand for PPAR-γ (10). The above findings coupled with our ob-

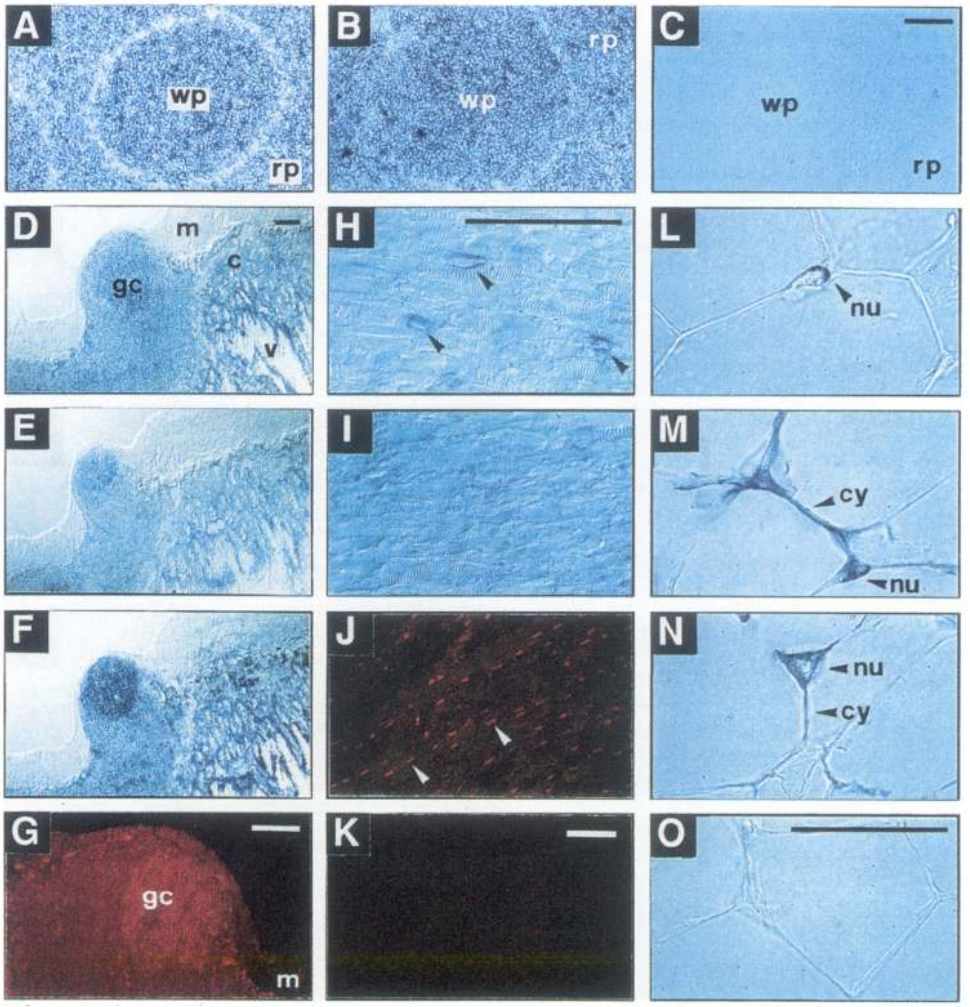

FIG. 5. Differential expression of rPPAR-α, -β, and -γ in spleen, Peyer's patches, heart, and white adipose tissue. A-C, Spleen. *In situ* hybridization. PPAR-γ (A) and -β (B) are abundantly expressed in white pulp (wp; lymphocyte proliferation center) as well as in red pulp (rp; erythrocyte phagocytosis centers). C, Sense control for PPAR-γ. D-G, Peyer's patches. *In situ* hybridization and immunohistochemistry. PPAR-α (D), -γ (E), and -β (F) are expressed in Peyer's patches (lymphoid nodes from ileum). Interestingly, level of expression of PPARs is strongest in germinative center (gc) of the patches, where undifferentiated B lymphocytes proliferate; c, crypts; m, muscular layers; v, villi. G, PPAR proteins are present in germinative center of Peyer's patches, confirming *in situ* hybridization results. H-K, Heart. *In situ* hybridization and immunohistochemistry. Antisense (H) and sense (I) probes for PPAR-α. PPAR-α transcript is concentrated in perinuclear zone of cardiomyocytes (H, *arrows*), as in hepatocytes (see Fig. 3F). By immunohistochemical analysis, PPAR proteins are observed in nuclei of cardiomyocytes (J, *arrows*). K, Control with preimmune serum. L-O, White adipose tissue (epididymal). *In situ* hybridization. PPAR-α (L) presents a low expression in perinuclear zone of adipocytes (nu). PPAR-γ (M) and PPAR-β (N) transcripts are much more abundant and located around nuclei (nu) as well as in the remaining cytoplasm (cy). O, Sense control for PPAR-γ. *Bars*, 100 μm; except L-O, 50 μm.

servation of high expression of PPAR-γ in the white adipose tissue substantiate the crucial role of PPAR-γ in adipogenesis. Our results further suggest a PPAR-γ function in the spleen.

PPAR transcripts are concentrated in the perinuclear region

The PPAR transcripts, when abundant, are concentrated in the perinuclear region of the cells. This is particularly obvious in cells having a large diameter, as illustrated by PPAR-α in hepatocytes (Fig. 3F), cardiomyocytes (Fig. 5H), and enterocytes (Fig. 4T) and by PPAR-β in Purkinje cells (Fig. 2H) and kidney cells (Fig. 3, A and C). Recently, a similar perinuclear localization of transcripts was described for another member of the nuclear receptor superfamily, the estrogen receptor, that is nuclear (30–32). We showed by immunohistochemical analysis that, as expected, the PPAR protein localization is essentially nuclear. One may speculate that the perinuclear localization of PPAR and estrogen receptor transcripts facilitates the nuclear translocation of the newly synthesized receptors.

Potential roles of PPARs

Important roles of PPARs in lipid metabolism have already been established in liver and adipose tissue (reviewed in Ref. 1). Our results suggest new directions of investigation for potential roles of PPARs in a range of other tissues.

PPARs are expressed in numerous cell populations that synthesize different proteins of the fatty acid binding protein family (FABPs). Hepatic FABP (L-FABP) and adipocyte aP2 genes have been shown to be controlled by PPAR-α (33) and PPAR-γ (18), respectively. In the intestine, the pattern of expression of PPARs (Fig. 4) corresponds to that of different members of the FABP family, particularly to L-FABP (34, 35) and cellular retinol binding protein II (36), whose genes may be controlled by PPARs in enterocytes. Indeed, a clofibrate-rich diet stimulates their transcription (35, 37). The regions of highest PPAR and FABP coexpression correspond to the regions of the digestive tract, where the major portion of dietary lipids is absorbed (triglycerides and phospholipids in the duodenum and jejunum and cholesterol in ileum). It is noteworthy that PPAR and FABP expressions are low in cecum and colon, where nutrient absorption is almost totally absent (this study and Refs. 35, 38). In the CNS, membrane lipids (phospholipids and cholesterol) confer to neurons and glial cells some of their electrical and physical properties. Apart from the CNS, PPARs are expressed in the choroid plexus, which synthesizes and secretes high amounts of apolipoproteins into the cerebrospinal fluid (39). Apolipoprotein E and apolipoproteins B-E receptors are responsible for

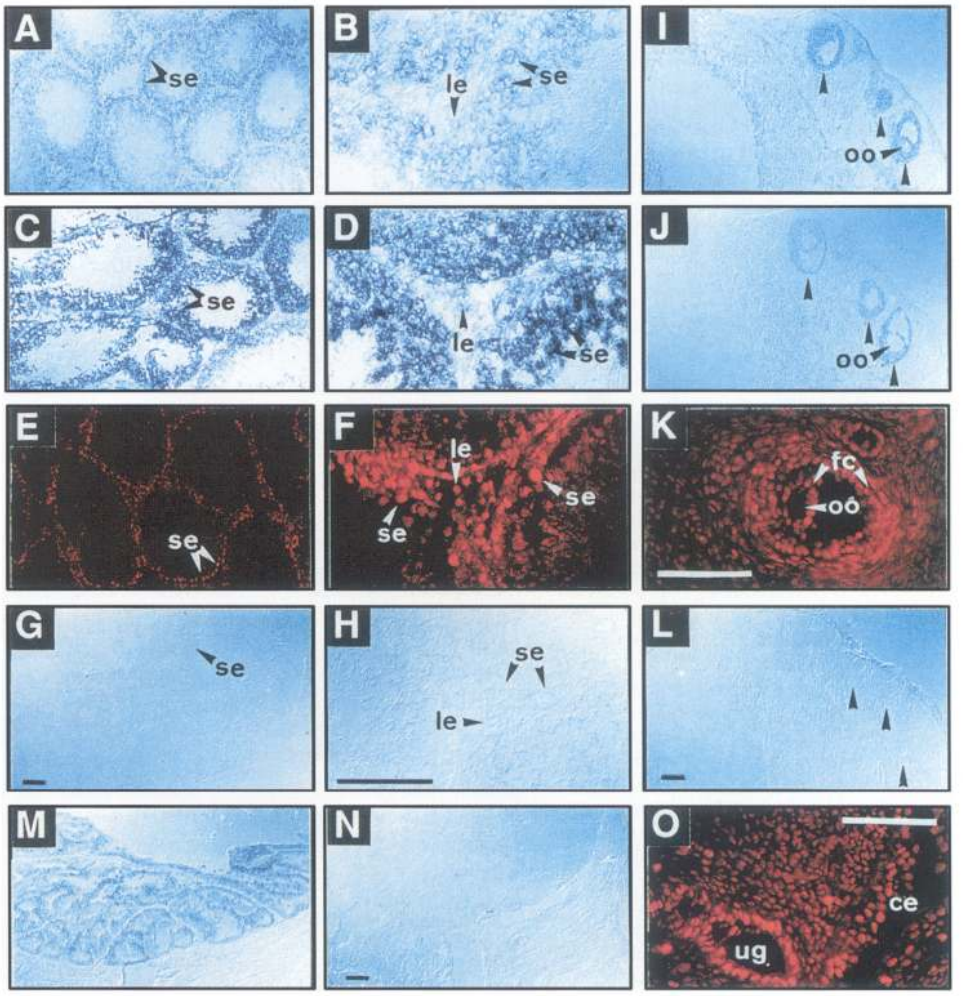

FIG. 6. Differential expression of rPPAR-α, -β, and -γ in genital system. A-H, Testis. *In situ* hybridization and immunohistochemistry. A and B, PPAR-α; C and D, PPAR-β; E and F, immune; G and H, sense control for PPAR-α. PPAR-β is very abundantly expressed in periphery of seminiferous tubules. PPAR-α presents a lower expression in the same cells. As shown by immunohistochemical analysis (G and H), PPARs are expressed in Sertoli (se) and Leydig (le) cells but are not detected in the germ line (spermatogonia to spermatozoan). I-L, Ovary. *In situ* hybridization and immunohistochemistry. PPAR-α (I) and -β (J) are expressed in different follicle stages (*arrows*). The same result is obtained by immunohistochemical analysis (K). In ovary, PPARs are expressed in follicular cells (fc) but are not detected in oocytes (oo). L, Sense control for PPAR-α. M and N, Seminal gland. *In situ* hybridization. Antisense (M) and sense (N) probes for PPAR-β. PPARs are present in mucosal epithelium of seminal gland. O, Uterus. Immunohistochemistry. PPAR proteins are observed in nuclei of epithelial cells of the uterine glands (ug), as well as cells of the cervix (ce; uterine mucosa). *Bars*, 100 μm.

membrane remodeling and fatty acid trafficking and recycling in the CNS (40). It will be of interest to analyze the potential regulation of their genes by PPARs, as it has already been demonstrated that apolipoproteins A-I, A-II, and C-III are regulated by PPARs (41–43). The recent discovery that lipoprotein lipase is directly regulated by PPARs (Schoonjans K, Staels B, Deeb S, Auwerx J, submitted for publication) may argue for PPAR participation in the immune system energy metabolism. Indeed, these receptors, particularly PPAR-γ, are well expressed in lymphocyte proliferation centers of the spleen and the Peyer's patches, which synthesize and secrete high amounts of lipoprotein lipase to recrute circulating fatty acids as a major source of fuel (44). We observed the expression of PPARs in numerous tissues that produce high amounts of arachidonic acid (cerebellum, hippocampus, distal part of the nephron, stomach, and immune and genital systems). This fatty acid is a potent activator of PPARs (8, 9) and, together with its metabolites (prostaglandins, leukotrienes, and thromboxanes), plays important roles in the signaling pathways of all cells. Arachidonic acid is mainly produced by the action of phospholipases A2 and C and diacylglycerol lipase. Investigation of the potential regulation of these genes by PPARs would be of great interest.

Little is known about the roles of PPARs in cell differentiation. Recent studies indicate that PPAR-γ can stimulate adipose differentiation in cultured fibroblasts (16). PPAR may also participate in epidermal keratinocyte differentiation, and particularly in the establishment of the functional lipid barrier of the skin (45). In our experiments, no expression of PPARs was observed in the adult epidermis, except in hair follicles and sebaceous glands for PPAR-α and -β. One would expect that the action of PPARs in the establishment of the lipid barrier in the stratified epidermis should take place during embryonic development, between E15 and E18 (45). Thus, the analysis of the developmental expression of PPARs will be of particular interest and will probably reveal specific and transient involvements of these receptors in many developmental and differentiation processes.

Conclusions

We have described the expression patterns of the three different forms of PPARs in the rat. PPAR-α is strongly expressed in cells with high catabolic rates of fatty acids and high peroxisomal metabolism (hepatocytes, cardiomyocytes, proximal tubules of kidney, and intestinal mucosa). PPAR-β is abundantly and ubiquitously expressed, whereas PPAR-γ presents a much more restricted expression (retina, immune system, and white adipose tissue). The fact that PPARs are coexpressed with differential levels of expression in most of

the tissues studied, in addition to their their capacity to bind identical response elements, suggests specific roles for these receptors in the regulation of similar sets of genes. If this were true, their differential activation by distinct molecules would represent a key regulatory step. Thus, variations of tissue expression of the different forms of PPARs in concert with variations in the distribution of their specific ligands or activators would lead to multiple possible combinations of fine tuning for the stimulation or the repression of target genes.

Acknowledgments

We thank E. Jeannin for cell culture and transfections; B. Corthésy for helpful discussion; and B. Desvergne, P. Devchand, and G. Krey for a critical reading of the manuscript. We are grateful to S. Green for the mPPAR-α/pSG5 plasmid, P. Grimaldi for the mPPAR-β/pSG5 plasmid, R.M. Evans for the mPPAR-γ/pSG5 plasmid, and K. Ozato for the mRXR-β/pSG5 plasmid.

References

1. **Wahli W, Braissant O, Desvergne B** 1995 Peroxisome proliferator-activated receptors: transcriptional regulators of adipogenesis, lipid metabolism and more . . . Chemistry & Biology 2:261–266
2. **Desvergne B, Wahli W** 1995 PPAR: a key nuclear factor in nutrient/gene interactions? In: Bauerle P (ed) Inducible Transcription. Birkhäuser, Boston, MA, vol 1:142–176
3. **Dreyer C, Krey G, Keller H, Givel F, Helftenbein G, Wahli W** 1992 Control of the peroxisomal beta-oxidation pathway by a novel family of nuclear hormone receptors. Cell 68:879–887
4. **Kliewer SA, Forman BM, Blumberg B, Ong ES, Borgmeyer U, Mangelsdorf DJ, Umesono K, Evans RM** 1994 Differential expression and activation of a family of murine peroxisome proliferator-activated receptors. Proc Natl Acad Sci USA 91:7355–7359
5. **Sher T, Yi HF, McBride OW, Gonzalez FJ** 1993 cDNA cloning, chromosomal mapping, and functional characterization of the human peroxisome proliferator activated receptor. Biochemistry 32: 5598–5604
6. **Schmidt A, Endo N, Rutledge SJ, Vogel R, Shinar D, Rodan GA** 1992 Identification of a new member of the steroid hormone receptor superfamily that is activated by a peroxisome proliferator and fatty acids. Mol Endocrinol 6:1634–1641
7. **Issemann I, Green S** 1990 Activation of a member of the steroid hormone receptor superfamily by peroxisome proliferator. Nature 347:645–650
8. **Göttlicher M, Widmark E, Li Q, Gustafsson J-Å** 1992 Fatty acids activate a chimera of the clofibric acid-activated receptor and the glucocorticoid receptor. Proc Natl Acad Sci USA 89:4653–4657
9. **Keller H, Dreyer C, Medin J, Mahfoudi A, Ozato K, Wahli W** 1993 Fatty acids and retinoids control lipid metabolism through activation of peroxisome proliferator-activated receptor-retinoid X receptor heterodimers. Proc Natl Acad Sci USA 90:2160–2164
10. **Lehmann JM, Moore LB, Smith-Oliver TA, Wilkison WO, Willson TM, Kliewer SA** 1995 An antidiabetic thiazolidinedione is a high affinity ligand for the nuclear receptor PPARγ. J Biol Chem 270: 12953–12956
11. **Hinton RH, Price SC** 1993 Extrahepatic peroxisome proliferation and the extrahepatic effects of peroxisome proliferators. In: Gibson G, Lake B (eds) Peroxisomes: Biology and Importance in Toxicology and Medicine. Taylor and Francis, London, pp 487–511
12. **Zaar K** 1992 Structure and function of peroxisomes in the mammalian kidney. Eur J Cell Biol 59:233–254
13. **Cablé S, Kedinger M, Dauça M** 1993 Peroxisomes and peroxisomal enzymes along the crypt-villus axis of the rat intestine. Differentiation 54:99–108
14. **Auestad N, Korsak RA, Morrow JW, Edmond J** 1991 Fatty acid oxidation and ketogenesis by astrocytes in primary culture. J Neurochem 56:1376–1386
15. **Chawla A, Schwarz EJ, Dimaculangan DD, Lazar MA** 1994 Peroxisome proliferator-activated receptor (PPAR) gamma: adipose-predominant expression and induction early in adipocyte differentiation. Endocrinology 135:798–800
16. **Tontonoz P, Hu E, Spiegelman BM** 1994 Stimulation of adipogenesis in fibroblasts by PPARγ2, a lipid-activated transcription factor. Cell 79:1147–1156
17. **Zhu Y, Alvarez K, Huang Q, Rao SM, Reddy JK** 1993 Cloning of a new member of the peroxisome proliferator activated receptor gene family from mouse liver. J Biol Chem 268:26817–26820
18. **Tontonoz P, Hu E, Graves RA, Budavari AI, Spiegelman BM** 1994 mPPARγ2, tissue-specific regulator of an adipocyte enhancer. Genes Dev 8:1224–1234
19. **Lemberger T, Staels B, Saladin R, Desvergne B, Auwerx J, Wahli W** 1994 Regulation of the peroxisome proliferator activated receptor α gene by glucocorticoids. J Biol Chem 269:24527–24530
20. **Crowe JS, Cooper HJ, Smith MA, Sims MJ, Parker D, Gewert D** 1991 Improved cloning efficiency of polymerase chain reaction (PCR) products after proteinase K digestion. Nucleic Acids Res 19:184
21. **Amri E-Z, Bonino F, Ailhaud G, Abumrad NA, Grimaldi PA** 1995 Cloning of a protein that mediates transcriptional effects of fatty acids in preadipocytes. Homology to peroxisome proliferator-activated receptors. J Biol Chem 270:2367–2371
22. **Kainu T, Wikström A-C, Gustafsson J-Å, Pelto-Huikko M** 1995 Localization of the peroxisome proliferator-activated receptor in the brain. NeuroReport 5:2481–2485
23. **Kliewer SA, Umesono K, Noonan DJ, Heyman RA, Evans RM** 1992 Convergence of 9-cis retinoic acid and peroxisome proliferator signalling pathways through heterodimer formation of their receptors. Nature 358:771–774
24. **Mangelsdorf DJ, Borgmeyer U, Heyman RA, Zhou JY, Ong ES, Oro AE, Kakizuka A, Evans RM** 1992 Characterization of three RXR genes that mediate the action of 9-cis retinoic acid. Genes Dev 6:329–344
25. **Tontonoz P, Hu E, Devine J, Beale EG, Spiegelman BM** 1995 PPARγ2 regulates adipose expression of the phosphoenolpyruvate carboxykinase gene. Mol Cell Biol 15:351–357
26. **Krey G, Keller H, Mahfoudi A, Medin J, Ozato K, Dreyer C, Wahli W** 1993 Xenopus peroxisome proliferator activated receptors: genomic organization, response element recognition, heterodimer formation with retinoid X receptor and activation by fatty acids. J Steroid Biochem Mol Biol 47:65–73
27. **Reddy JK, Rao MS, Moody DE, Qureshi SA** 1976 Peroxisome development in the regenerating pars recta (P3 segment) of proximal tubules of the rat kidney. J Histochem Cytochem 24:1239–1248
28. **Lee SST, Pineau T, Drago J, Lee EJ, Owens JW, Kroetz DL, Fernandez-Salguero PM, Westphal H, Gonzalez FJ** 1995 Targeted disruption of the α isoform of the peroxisome proliferator-activated receptor gene in mice results in abolishment of the pleiotropic effects of peroxisome proliferators. Mol Cell Biol 15:3012–3022
29. **Jow L, Mukherjee R** 1995 The human peroxisome proliferator-activated receptor (PPAR) subtype NUC1 represses the activation of hPPAR alpha and thyroid hormone receptors. J Biol Chem 270: 3836–3840
30. **Koji T, Brenner RM** 1993 Localization of estrogen receptor messenger ribonucleic acid in rhesus monkey uterus by nonradioactive *in situ* hybridization with digoxigenin-labeled oligodeoxynucleotides. Endocrinology 132:382–392
31. **King WJ, Greene GL** 1984 Monoclonal antibodies localize oestrogen receptor in the nuclei of target cells. Nature 307:745–747
32. **Welshons WV, Lieberman ME, Gorski J** 1984 Nuclear localization of unoccupied oestrogen receptors. Nature 307:747–749
33. **Issemann I, Prince R, Tugwood J, Green S** 1992 A role for fatty acids and liver fatty acid binding protein in peroxisome proliferation? Biochem Soc Trans 20:824–827
34. **Roth KA, Rubin DC, Birkenmeier EH, Gordon JI** 1991 Expression of liver fatty acid-binding protein/human growth hormone fusion genes within the enterocyte and enteroendocrine cell populations of fetal transgenic mice. J Biol Chem 266:5949–5954
35. **Simon TC, Roth KA, Gordon JI** 1993 Use of transgenic mice to map cis-acting elements in the liver fatty acid-binding protein gene (FABPl) that regulate its cell lineage-specific, differentiation-

dependent, and spatial patterns of expression in the gut epithelium and in the liver acinus. J Biol Chem 268:18345–18358
36. **Crow JA, Ong DE** 1985 Cell-specific immunohistochemical localization of a cellular retinol-binding protein (type two) in the small intestine. Proc Natl Acad Sci USA 82:4707–4711
37. **Goda T, Yasutake H, Takase S** 1994 Dietary fat regulates cellular retinol-binding protein II gene expression in rat jejunum. Biochim Biophys Acta 1200:34–40
38. **Cohn S, Simon TC, Roth KM, Birkenmeier EH, Gordon JI** 1992 Use of transgenic mice to map cis-acting elements in the intestinal fatty acid binding protein gene (Fabpi) that control its cell lineage-specific and regional patterns of expression along the duodenal-colonic and crypt-villus axes of the gut epithelium. J Cell Biol 119:27–44
39. **Albers JJ, Tollefson JH, Wolfbauer G, Albright, Jr, RE** 1992 Cholesteryl ester transfer protein in human brain. Int J Clin Lab Res 21:264–266
40. **Pitas RE, Boyles JK, Lee SH, Hui D, Weisgraber KH** 1987 Lipoproteins and their receptors in the central nervous system. J Biol Chem 262:14352–14360
41. **Vu-Dac N, Schoonjans K, Laine B, Fruchart J-C, Auwerx J, Staels B** 1994 Negative regulation of the human apolipoprotein A-I promoter by fibrates can be attenuated by the interaction of the peroxisome proliferator-activated receptor with its response element. J Biol Chem 269:31012–31018
42. **Vu-Dac N, Schoonjans K, Kosykh V, Dallongeville J, Fruchart J-C, Staels B, Auwerx J** 1995 Fibrates increase human apolipoprotein A-II expression through activation of the peroxisome proliferator-activated receptor. J Clin Invest 96:741–750
43. **Hertz R, Bishara-Shieban J, Bar-Tana J** 1995 Mode of action of peroxisome proliferators as hypolipidemic drugs. Suppression of apolipoprotein C-III. J Biol Chem 270:13470–13475
44. **Calder PC Yaqoob P, Newsholme EA** 1994 Triacylglycerol metabolism by lymphocytes and the effect of triacylglycerols on lymphocyte proliferation. Biochem J 298:605–611
45. **Imakado S, Bickenbach JR, Bundman DS, Rothnagel JA, Attar PS, Wang X-J, Walczak VR, Wisniewski S, Pote J, Gordon JS, Heyman RA, Evans RM, Roop DR** 1995 Targeting expression of a dominant-negative retinoic acid receptor mutant in the epidermis of transgenic mice results in loss of barrier function. Genes Dev 9:317–329